Journal of Inflammation Research

Dovepress
Taylor & Francis Group

Open Access Full Text Article

ORIGINAL RESEARCH

PCK2, a SASP-Associated Gene, Serves as an Independent Prognostic Indicator in Diffuse Large B-Cell Lymphoma

Minggui Chen[1,*], Yueyuan Pan[2,*], Jinfang Zhang[3], Yan Zeng[1]

[1]Department of Precision Clinical Laboratory, Zhanjiang Central Hospital, Guangdong Medical University (Central People's Hospital of Zhanjiang), Zhanjiang, Guangdong, 524023, People's Republic of China; [2]Zhanjiang Institute of Clinical Medicine, Zhanjiang Central Hospital, Guangdong Medical University (Central People's Hospital of Zhanjiang), Zhanjiang, Guangdong, 524023, People's Republic of China; [3]Department of Pathology, Shenzhen Nanshan People's Hospital (NSPH), Shenzhen, Guangdong, 518052, People's Republic of China

*These authors contributed equally to this work

Correspondence: Yan Zeng, Precision Clinical Laboratory, Central People's Hospital of Zhanjiang, Guangdong Medical University Zhanjiang Central Hospital, Zhanjiang, 524037, People's Republic of China, Email yzeng910@163.com

Background: Diffuse large B-cell lymphoma (DLBCL) is characterised by substantial heterogeneity in phenotype and genetics. Recent studies have demonstrated that senescence-associated secretory phenotype (SASP) is both a tumor suppressor and a promoter of tumorigenesis and progression. However, reports on the effects of SASP on DLBCL remain limited. This study aimed to identify the SASP-related indicator of DLBCL, thereby providing new insights into the pathology of DLBCL.

Methods: Differential analysis and weighted co-expression network analysis (WGCNA) were applied to identify differentially expressed genes (DEGs) and key gene modules of DLBCL. Univariate Cox regression analysis was employed to identify SASP-related genes that serve as independent risk factors for DLBCL prognosis. Overlapped among three methods to obtain the hub gene and explore its potential mechanisms in DLBCL. The association between *PCK2* and disease heterogeneity in DLBCL was further analyzed. We constructed a co-expression network centered on *PCK2* and validated their expression and prognostic performance. Finally, 30 cases of tumour tissues were utilized to validate the expression of PCK2 in DLBCL patients by immunohistochemistry.

Results: In this study, through integrated bioinformatics methods, *PCK2* was identified as a SASP-related gene in DLBCL. *PCK2* can be regarded as a candidate indicator with good prognostic performance (AUC=0.953, Hazard Ratio (HR) =1.89, 95% CI=1.488–2.399, $p<0.001$). *PCK2* was notably associated with multiple disease characteristics in DLBCL, particularly the immunosuppressive microenvironment and SASP signal. Furthermore, genes exhibiting high correlation with *PCK2* demonstrated significant predictive value for DLBCL prognosis. Through immunohistochemistry, it was verified that PCK2 was markedly upregulated in DLBCL compared to normal controls.

Conclusion: As a SASP-related gene, *PCK2* serve as a candidate indicator providing supplementary information for DLBCL disease monitoring and prognostic assessment.

Keywords: DLBCL, SASP, PCK2, Tumor immune microenvironment, Glycolysis

Introduction

DLBCL, as the predominant subtype of non-Hodgkin lymphoma (NHL),[1,2] around 40% of patients with DLBCL develop refractory or relapsed disease, which is considered as the ultimate cause of mortality in this population.[3] Despite extensive investigations into various risk factors, the exact etiology, optimal therapeutic strategies, and prognostic outcomes of DLBCL remain elusive.[4] In the face of these challenges, identifying more delicate biomarkers of DLBCL is crucial.

The progression and prognosis of DLBCL are influenced by multiple factors. Based on cell of origin classification and oncogenic mechanisms, DLBCL is divided into three subgroups: germinal-center B-cell-like (GCB), activated

Received: 18 June 2025
Accepted: 6 November 2025
Published: 20 November 2025

B-cell-like (ABC), and unclassified subtypes.[5] Patients with GCB subtype exhibit both superior overall survival (OS) and progression-free survival compared with ABC subtype patients.[6] Tumor cells have implemented certain metabolic adjustment to shield themselves from nutrient scarcity. Even in the presence of oxygen, glucose is still converted by a cascade of enzymes into lactate instead of being fully oxidized to carbon dioxide, a process termed aerobic glycolysis, or the Warburg effect,[7] which also constitutes a core metabolic hallmark of DLBCL. Recent study has uncovered metabolic and immune microenvironmental heterogeneity in DLBCL. Tumors with high glycolytic activity display an immunosuppressive milieu, and seven glycolysis-related genes with robust prognostic value have been identified. Moreover, highly aggressive DLBCL is characterized by abundant infiltration of interferon activated tumor associated macrophages (IFN_TAMs), which portends poor prognosis, and recognized their specific molecular markers.[8]

Several studies have indicated that Cellular senescence (CS) is implicated in various critical processes, particularly in cancer.[9] Senescent cells are not quiescent, they develop a complex senescence-associated secretory phenotype (SASP), characterized by the sustained release of numerous bioactive molecules.[10] Based on the function of factors, SASP can be broadly grouped into the five categories: cytokines (eg, IL-6, IL-1β), chemokines (eg, CXCL1, CXCL16), proteases (eg, MMP-12, MMP-14), growth factors (eg, VEGF-A, GDF-15), and membrane proteins/receptors (eg, DPP4, ICAM-1).[11] It was confirmed that the effect of SASP on tumors is dual-edged.[12] SASP exerts protective effects against tumorigenesis by maintaining cell cycle arrest and recruiting immune cells to eradicate defective or oncogenic cells.[10,13–15] However, emerging evidence suggests that SASP functions as a tumor driver by promoting tumor cell proliferation and inducing epithelial-mesenchymal transition (EMT).[16–18] The essential pro-tumor function of SASP lies in its reshaping the tumor immune microenvironment (TIME). SASP can accumulate immunosuppressive cells to avert immune purging of tumor cells while also modulating the expression of immune checkpoints that further construct an immunosuppressive microenvironment.[19,20] Interestingly, in tumor cells, lactate accumulated through Warburg effect induced DNA damage via the NOX1-ROS axis, thereby activating NF-κB and driving the SASP.[21,22] Despite substantial progress in SASP-tumor research, the precise mechanisms mediating its impact on DLBCL pathogenesis remain incompletely characterized. In our analysis, SASP signal was markedly elevated in DLBCL patients compared with controls. However, SASP program is heterogeneous, and its composition is shaped by cell type, genetic background, and senescence inducing stimuli.[23] Therefore, investigating SASP-related genes in DLBCL is of great significance.

PCK2 is one of the isoform of phosphoenolpyruvate carboxykinase (PEPCK), it's an essential gluconeogenic catalyst, exerts pivotal control over cellular energy homeostasis.[24] PCK2 had been consistently linked to the progression of multiple solid tumors. Under glucose deprived conditions, PCK2 can stimulate the anaplerosis of the tricarboxylic acid (TCA) cycle, and drove the production of phosphoenolpyruvate (PEP) from glutamine to achieve glucose independent tumor growth.[25] Moreover, PCK2 can modulate the mTOR pathway, serine metabolism, and remodel of TIME to drive the tumor growth and invasion.[26–28]

Considering the importance of SASP in DLBCL, recognizing SASP-related genes could be highly meaningful. This study utilized integrated bioinformatics approaches, combining immune infiltration analysis and clinical sample validation, to identify the SASP-related genes and elucidate its association with disease characteristics, which provided a candidate indicator of DLBCL and furnish testable hypotheses for follow up mechanistic studies.

Methods

Data Acquisition and Processing

In this study, we systematically searched for microarray research of DLBCL from the public Gene Expression Omnibus (GEO) dataset. Gene expression profiles of DLBCL and normal controls were obtained from GSE12453 (comprising 11 DLBCL patients and 25 normal controls).[29] GSE10846 (contained 414 DLBCL patients)[6] and GSE181063[30] (contained 1170 DLBCL patients) were used as the validation sets to investigate the relationship between SASP-related genes and prognostic characteristics of DLBCL. All cohorts have been normalized. The detailed processing pipeline was as follows: we downloaded the series matrix files from the GEO database, confirmed that the submitters had already performed normalization, applied a Log2 transformation, and used the "removeBatchEffect" function in the "Limma" package to correct for batch effects before including the data in downstream analyses. The SASP gene set was acquired from Genecards (https://www.genecards.org/). We retrieved gene list by searching the keyword "senescence-associated

secretory phenotype" and filtered candidates using a relevance score > 1.[31,32] Finally, 440 SASP-related genes were selected for subsequent analyses.

Differential and Enrichment Analyses

Applying R software to analyze the microarray profiles. GSE12453 was used to investigate the differential expression signature of DLBCL. Utilizing "FactoMineR" and "Factoextra" packages to conduct the principal component analysis (PCA).[33] The differentially expressed genes (DEGs) of DLBCL were explored using the package "Limma".[34] Employing the package "ClusterProfiler" to perform the enrichment analysis.[35] The "ggplot2" package was used to generate images for visualization.

WGCNA Analysis

Using the "WGCNA" package to conduct the WGCNA analysis, which was used to clarify the crucial gene module of DLBCL.[36] A total of 5290 genes, ranked in the top 25% by variation, were analyzed. A soft threshold of 20 (R^2=0.9) was chosen as the optimal value for constructing a stable scale-free network. Dynamic tree-cutting algorithm was employed to aggregate genes with similar biological characteristics into the same module. Based on the correlation coefficients, we selected the top two modules for further investigation.

Univariate Cox Regression Analysis

Univariate analysis was employed to assess the effect of individual covariates (predictor variables) on survival time using by "survival" package. We used Cox analysis to explore the significance of SASP-related gene set on the prognosis of DLBCL in GSE10846, and selected genes with Hazard Ratio (HR) >1.6 for subsequent analysis.

Identified the SASP-Related Gene of DLBCL

Genes obtained from the above three methods were intersected, and the result was visualized using a Venn diagram. The overlapping gene *PCK2* was regarded as the SASP-related gene of DLBCL. GEPIA database was utilized to clarify the *PCK2* expression between normal controls and DLBCL in TCGA dataset. Human Protein Atlas (HPA) dataset was applied to investigate the subcellular localization of PCK2. Package "pROC" was applied to construct the ROC curve.[37]

Prognostic Character Analysis

GSE10846 and GSE181063 were employed to validate the prognostic value of hub gene in DLBCL. Package "ggrisk" was employed to construct the risk score scatterplot. Using the "timeROC" package to construct the time-dependent ROC curve. The "Survival" package was utilized to generate the KM survival curve.

Identification the Potential Role of Hub Gene in DLBCL

Using median expression level of *PCK2* as the stratification threshold, the GSE10846 cohort was divided into two distinct subgroups (*PCK2*-High and *PCK2*-Low). We identified DEGs between two groups and conducted enrichment analysis. In the GO and KEGG analyses, items with adjusted p-value < 0.05 were considered significantly enriched. For GSEA analysis, items with FDR< 0.25 were regarded as critical enriched.

Immune Microenvironment Analysis

"Estimate" algorithm was utilized to investigate the relevance of *PCK2 and the* overall immune landscape.[38] Further evaluation of immune score was conducted between the *PCK2*-High and PCK2-Low groups.

Single-Sample GSEA (ssGSEA) Based Quantification of Pathway Activities

Using the ssGSEA approach, we quantified the enrichment of three gene sets across the samples. The SASP and immune-related signatures were obtained from the Molecular Signatures Database (MSigDB), the IFN_TAMs gene set were obtained from the literature.[8] Using the "GSVA" package, ssGSEA was conducted to calculate enrichment scores from rank transformed gene expression data, thereby estimating pathway activity in each samples.[39]

Construct the Correlation Network of Hub Gene

Correlation analysis was performed using the "Corrplot" package. We used the Spearman test to assess the correlation of each gene with PCK2, and the top 50 (positive and negative) genes were incorporated into the subsequent analysis.

Through STRING database, we systematically mapped interaction networks among 50 gene-encoded proteins, with subsequent visualization conducted in Cytoscape. The top five hub genes within the network were subsequently determined through the utilization of the cytohubba embedded.

Collection of Clinical Samples

The acquisition and utilization of the samples were in accordance with the principles of the declaration of Helsinki. 30 cases of DLBCL tumour tissues and 30 cases of reactive hyperplastic tissues from 2024 to 2025 were collected by pathology department at Central People's Hospital of Zhanjiang, which were used to verify the differences in PCK2 expression between the two groups.

Immunohistochemical (IHC) Staining

After excising the tissue specimen, proceed with dehydration, clearing, and infiltration. Fix the specimen in 4% paraformaldehyde, then place it in an automatic dehydrator for dehydration. Paraffin embedding and tissue sections: The sections are approximately 3 micrometers thick. Antigen exposure: Incubate with sodium citrate buffer under high pressure for 15 minutes. Blocking, primary antibody incubation, and secondary antibody incubation. Counterstain cell nuclei with hematoxylin solution. Observe the samples under an optical microscope, capture images at appropriate magnifications and fields. Perform statistical analysis using Image Pro Plus software for data quantification. The antibodies used for immunohistochemistry and their working concentrations are as follows: PCK2 antibody (Proteintech, Cat No:67676-1-Ig):1:500.

Statistical Analysis

Statistical analyses in R were performed using the "corr.test" function, and images were generated by "ggplot2". SPSS 19.0 was used for statistical analysis. Selection of independent samples *t*-test or Mann–Whitney *U*-test based on whether the sample conformed to a normal distribution and the variances between groups were equal. All data were presented as mean ± standard error of the mean (SEM). The images were edited using Adobe Photoshop (PS) 2022 software.

Results

The Workflow of Study

The workflow of this study is as follows: differential analysis and WGCNA were performed to obtain DEGs and key gene modules of DLBCL. Univariate Cox regression analysis was applied to identify SASP-related genes with independent prognostic values on DLBCL. The hub gene was recognized through the overlap of the three methods and its correlation with DLBCL disease characteristics was explored, including TIME, clinical traits, and SASP program. Additionally, through correlation analysis and protein-protein interaction (PPI) screening, we identified five genes highly associated with *PCK2* and validated their expression and prognostic effects in DLBCL. Finally, we evaluated the expression of PCK2 in DLBCL clinical samples by immunohistochemistry (Figure 1).

Analysis of DEGs and Their Potential Effect in DLBCL

GSE12453 was used to identify the DEGs between DLBCL and normal controls. Initially, PCA algorithm inferred that the global gene expression profiles of the two groups showed biological differences (Figure 2A). Genes that were characterized by adjusted p-value < 0.05 and |log2 FC| >1 were regarded as DEGs. A total of 1,110 DEGs were explored, with 974 upregulated and 136 downregulated (Figure 2B and C). GO analysis supported that these DEGs were implicated in multiple biological pathways, like "respiratory electron transport chain", and "oxidative phosphorylation" (Figure 2D). KEGG analysis defined significant enrichment in pathways such as "Thermogenesis", "Ribosome", and "Oxidative phosphorylation" (Figure 2E).

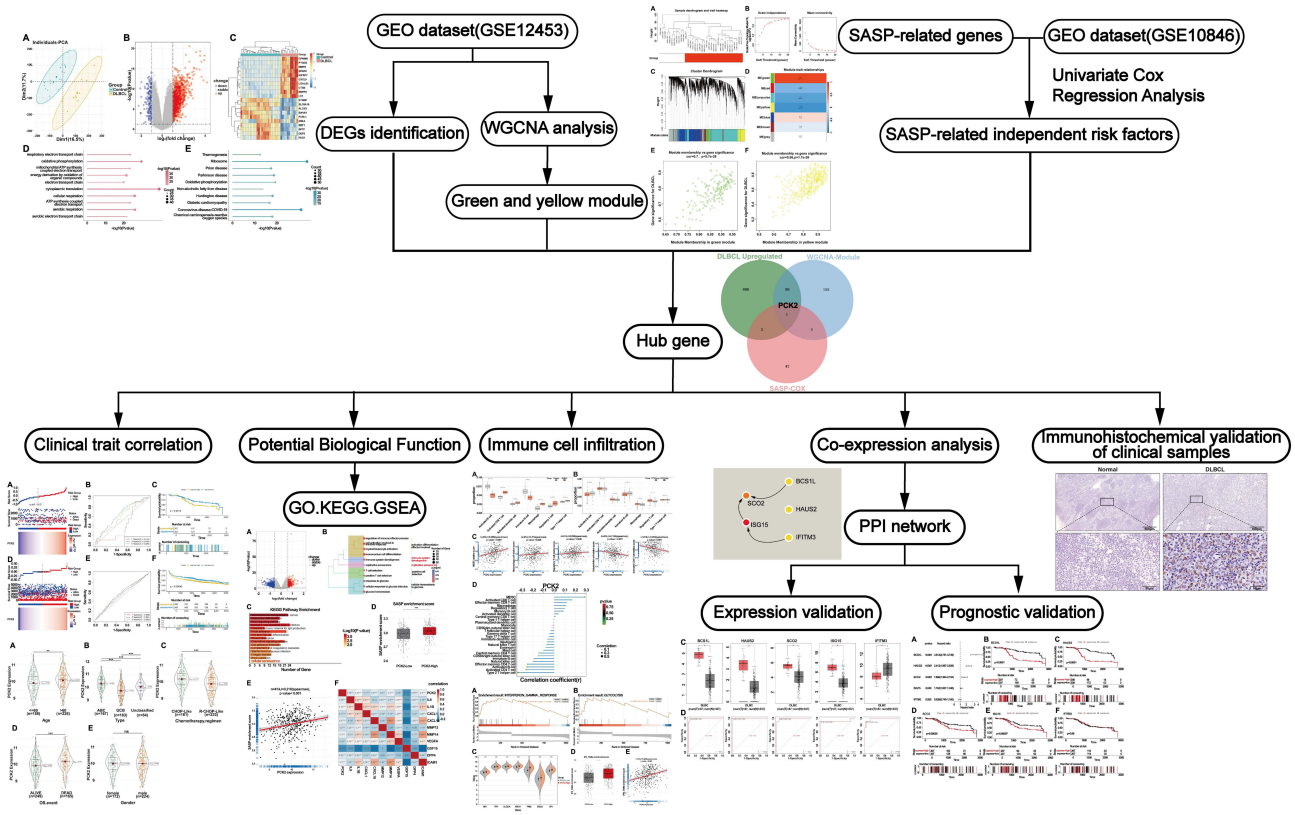

Figure 1 Flowchart of the study.

Identified the Essential Gene Modules of DLBCL by WGCNA

Critical gene modules associated with DLBCL were identified by WGCNA. Sample clustering tree without outliers (Figure 3A). In this study, genes with a coefficient of variation within the top 25% (totaling 5290 genes) were selected as input data for network construction. A robust co-expression network was established using the power of 20 (Figure 3B). Dynamic tree cutting algorithm was applied to identify and merge the similar modules, ultimately obtained 7 distinct gene modules (Figure 3C and D). Correlation analysis further revealed that MEgreen (cor=0.7) and MEyellow module (cor=0.66) were markedly related to DLBCL(Figure 3E and F). Therefore, genes that were characterized by gene significance (|GS|) >0.7 and module membership (|MM|) >0.7 in two modules were used for the subsequent analysis .

Identification the PCK2 as a Indicator of SASP Signature in DLBCL

Given the pivotal role of SASP in cancer, ssGSEA was utilized to assess the enrichment of SASP in DLBCL samples. Compared with the normal controls, SASP signal was markedly elevated in DLBCL (Figure 4A). To assess the prognostic significance of the SASP-related genes in DLBCL, univariate analysis was conducted using the GSE10846 dataset, and a forest plot was generated for the top 50 genes with the highest hazard ratios (HR) (Figure 4B). This study employed HR >1.6 as the statistical criterion to verify clinically significant risk factors associated with DLBCL progression. *PCK2* was identified by overlapping the upregulated of DEGs, genes in critical modules, and SASP-related genes with HR>1.6, which was considered to be a SASP-characterized indicator in DLBCL (Figure 4C). In TCGA dataset, *PCK2* was similarly found to be highly expressed in DLBCL (Figure 4D). ROC curve proved that *PCK2* had a good evaluate performance for DLBCL (Figure 4E). We used the HPA database to examine the subcellular localization of PCK2 in cells. PCK2 is mainly located in mitochondria (Figure 4F).

https://doi.org/10.2147/JIR.S548070

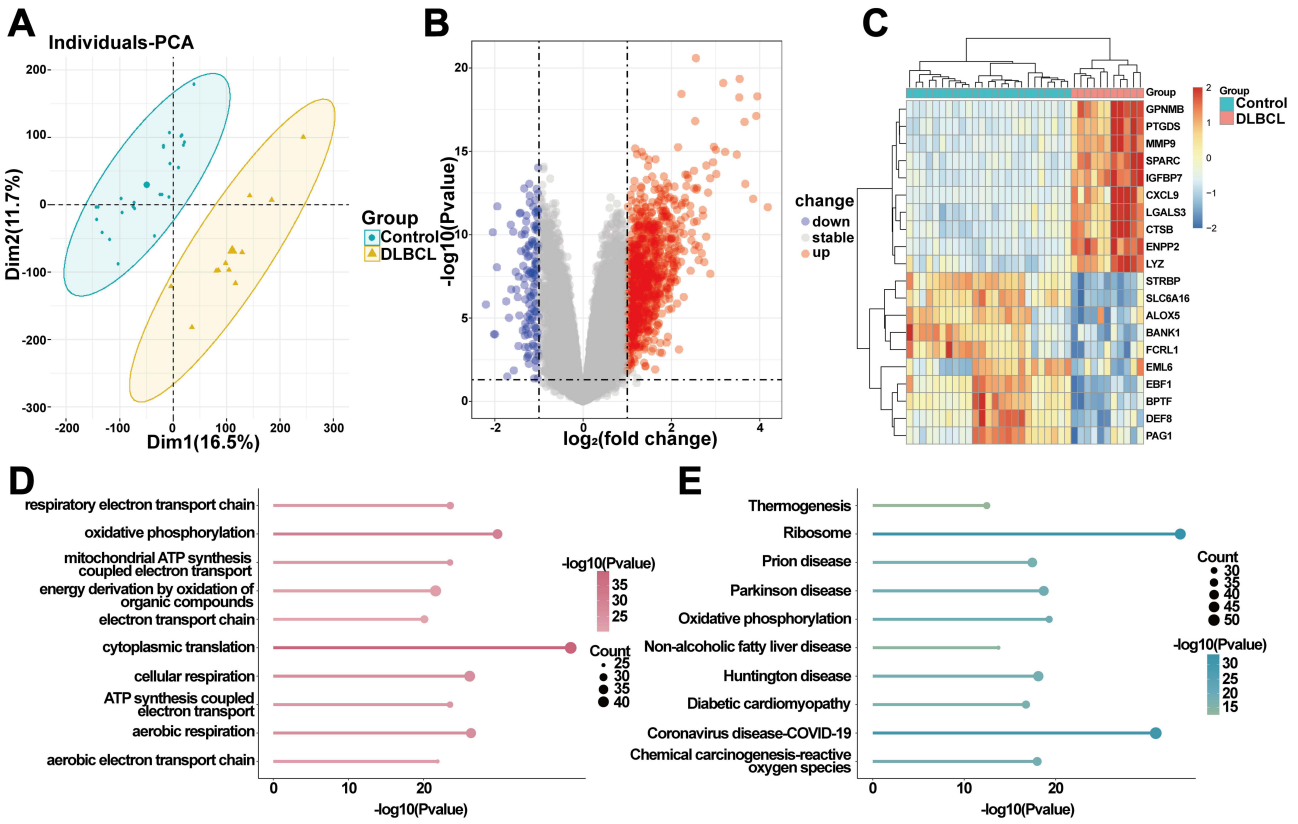

Figure 2 Differential and enrichment analysis of GSE12453. (**A**) PCA showing heterogeneous global gene expression profiles between the two groups. (**B**) The volcano plot visualizes DEGs in the GSE12453 dataset, with red markers indicating upregulated genes and blue markers denoting downregulated genes. (**C**) Heatmap showing the top 20 DEGs (upregulated and downregulated). (**D** and **E**) Enrichment analyses indicated the function of DEGs.

Validation the Prognostic Value of PCK2 in DLBCL

Above study has shown that PCK2 could serve as a candidate indicator for DLBCL. We systematically validated the prognostic characteristics of *PCK2* in DLBCL through multi-methodological assessments, including risk factor analysis, time-dependent ROC evaluation, and survival analysis constructed from the GSE10846 dataset (Figure 5A–C). Validation in cohort GSE181063 (n=1,170 DLBCL patients) confirmed PCK2 prognostic significance in DLBCL, demonstrating consistent associations with outcomes as observed in training cohort GSE10846 (Figure 5D–F).

PCK2 Was Strongly Associated with Multiple Clinical Traits of DLBCL

Using the GSE10846 dataset, we confirmed correlations between *PCK2* expression and multiple molecular characteristics of DLBCL. Age > 60 years and ABC subtype constitute unfavorable prognostic indicators for DLBCL in the clinic.[6,40–42] Compared with patients aged ≤60 years, *PCK2* expression was notably upregulated in those older than 60 years (Figure 6A). Notably, compared with ABC subtype, *PCK2* levels were substantially lower in GCB subtype (Figure 6B). The current study showed that R-CHOP significantly improves prognosis versus CHOP alone[43] Relative to CHOP treatment, *PCK2* was significantly down-regulated in the R-CHOP group (Figure 6C). Furthermore, *PCK2* was associated with survival outcome and was markedly elevated in patients whose overall survival status was documented as deceased (Figure 6D). However, no significant association was observed between *PCK2* and sex (Figure 6E).

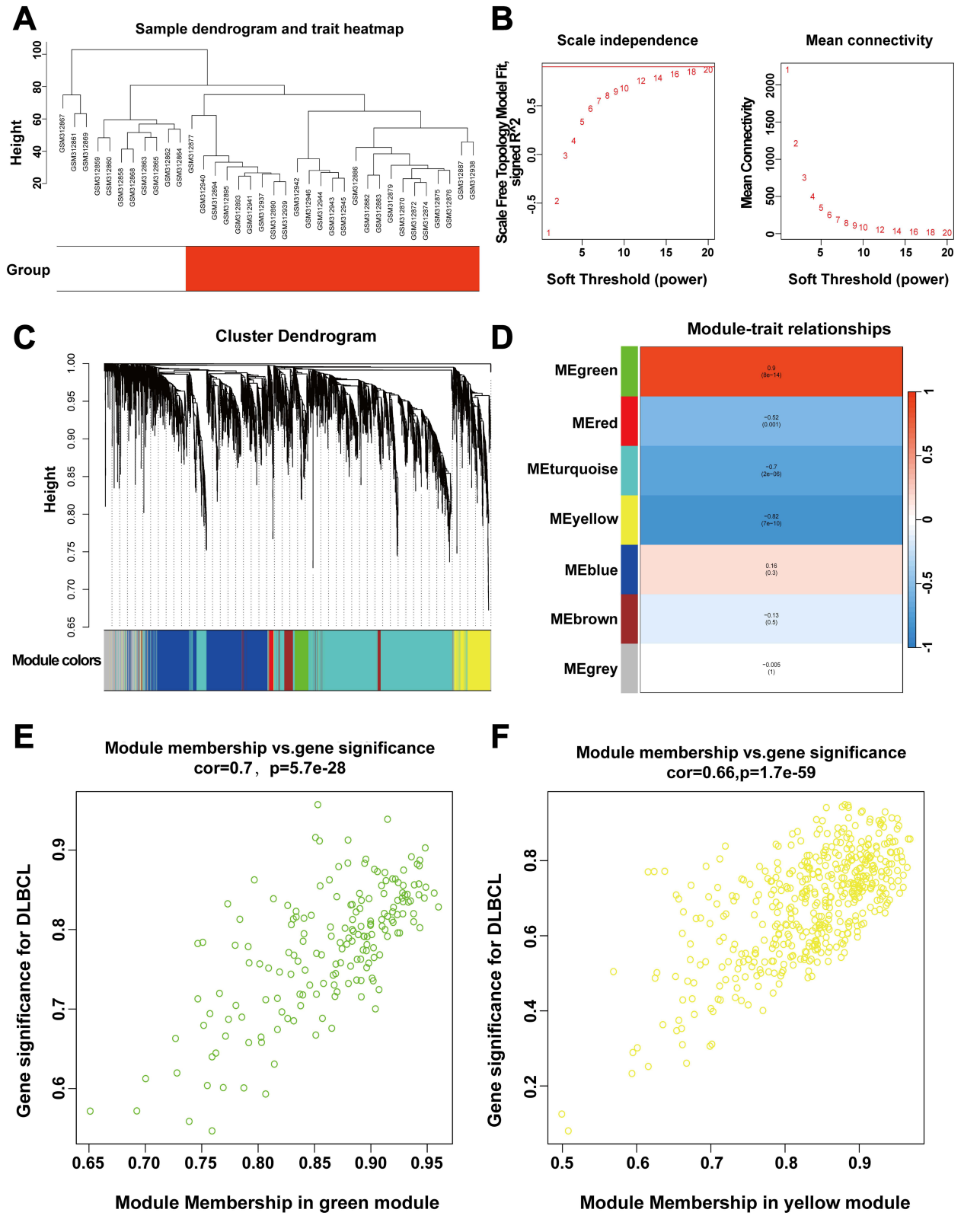

Figure 3 WGCNA analysis of GSE12453. (**A**) Constructing sample clustering trees to identify the presence of outliers. (**B**) Network topology analysis, selected the optimal soft threshold to establish a co-expression network. (**C**) Create a gene clustering tree using hierarchical clustering and dynamic tree cutting methods. (**D**) Heatmap indicating significant correlations between the top 2 modules (MEgreen, MEyellow) and DLBCL. (**E** and **F**) A scatterplot showing GS and MM for the green and yellow modules.

https://doi.org/10.2147/JIR.S548070

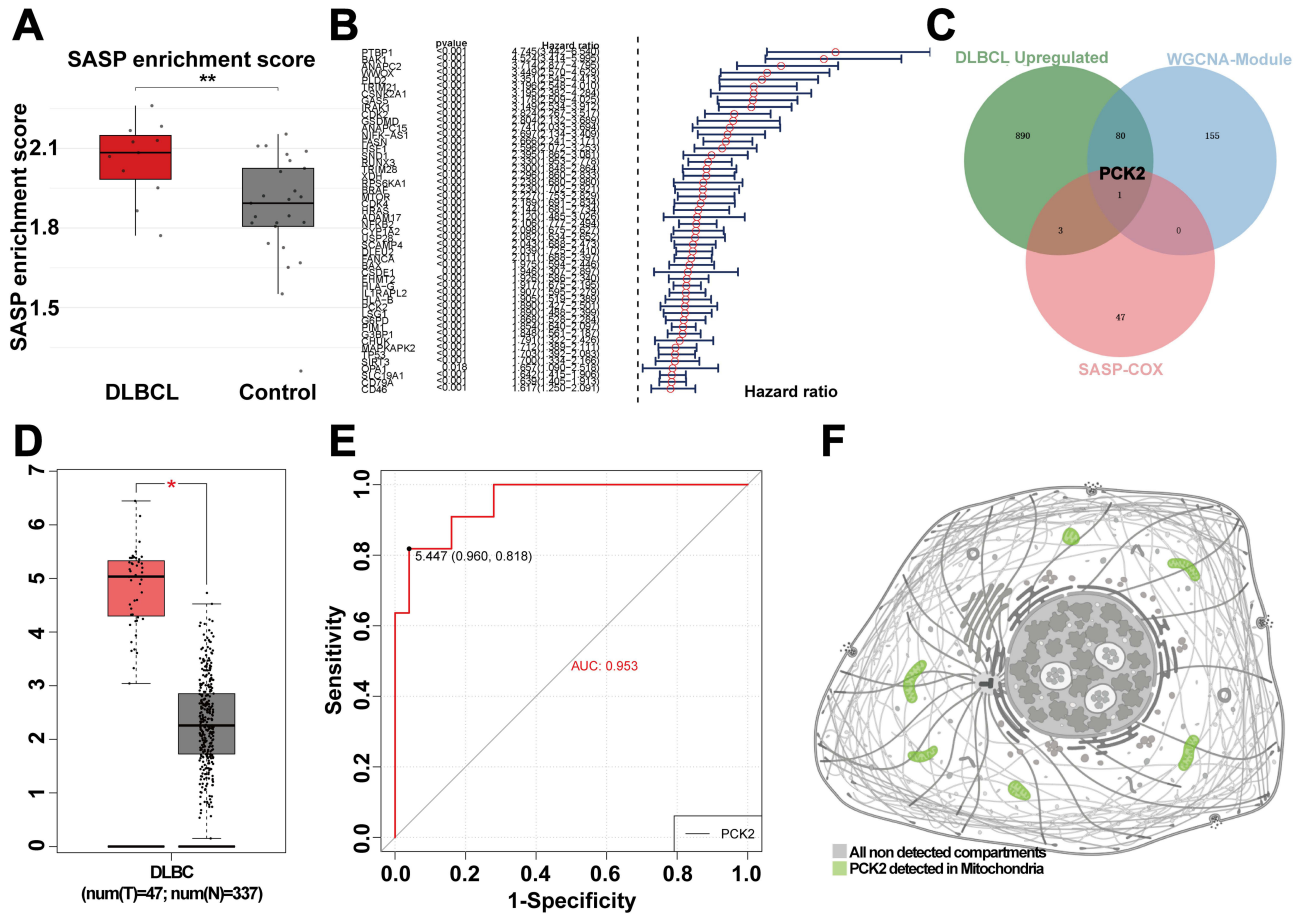

Figure 4 Identified the SASP-related genes in DLBCL. (**A**) Boxplot showing SASP enrichment scores of DLBCL and controls by ssGSEA. (**B**) Forest plot of HR (top 50 SASP-related genes) by univariate cox regression analysis from GSE10846. (**C**) Venn diagram displaying the key SASP-related gene explored by overlapping of three bioinformatics analysis methods. (**D**) Expression levels of PCK2 across groups in the DLBCL and normal control form TCGA dataset. (**E**) ROC curve was used to evaluate the AUC value of *PCK2* for DLBCL in GSE12453. (**F**) HPA database was utilized to determine the subcellular localization of PCK2. (*p<0.05, **p<0.01).

High Correlations Between PCK2 and SASP Signal in DLBCL

Using median expression level of *PCK2* as the stratification threshold, the GSE10846 cohort was divided into two distinct subgroups (*PCK2*-High and *PCK2*-Low). Differential expression analysis revealed 1123 genes with significant transcriptional changes, of which 417 were upregulated and 706 downregulated (Figure 7A). To examine the potential contributions of *PCK2* in DLBCL, enrichment analysis was conducted. GO and KEGG pathway enrichment analysis indicated that *PCK2* was markedly associated with "cellular senescence" pathway in DLBCL (Figure 7B and C). Given that the cellular senescence pathway is a principal driver of SASP and *PCK2* is an SASP-related gene, we next examined the relationship between *PCK2* and SASP signal in DLBCL. SASP enrichment score was markedly elevated in the *PCK2*-High group compared with the *PCK2*-Low group by ssGSEA, consistent with SASP activation in DLBCL patients (Figure 7D). Correlation analysis further revealed a significant positive correlation between *PCK2* and SASP signal (Figure 7E). What's more, *PCK2* showed robust associations with multiple canonical SASP markers (Figure 7F). The results established *PCK2* as tightly linked to the SASP program in DLBCL.

Relationship Between PCK2 and Immune Environment in DLBCL

Notably, immune-related pathways were significantly enriched by GSEA analysis (Figure 8A). We observed that *PCK2* was positively correlated with immune score by using the Estimate algorithms (Figure 8B). The immune score of the *PCK2*-High group was found to be markedly higher than *PCK2*-Low group (Figure 8C). As the important part of TIME,

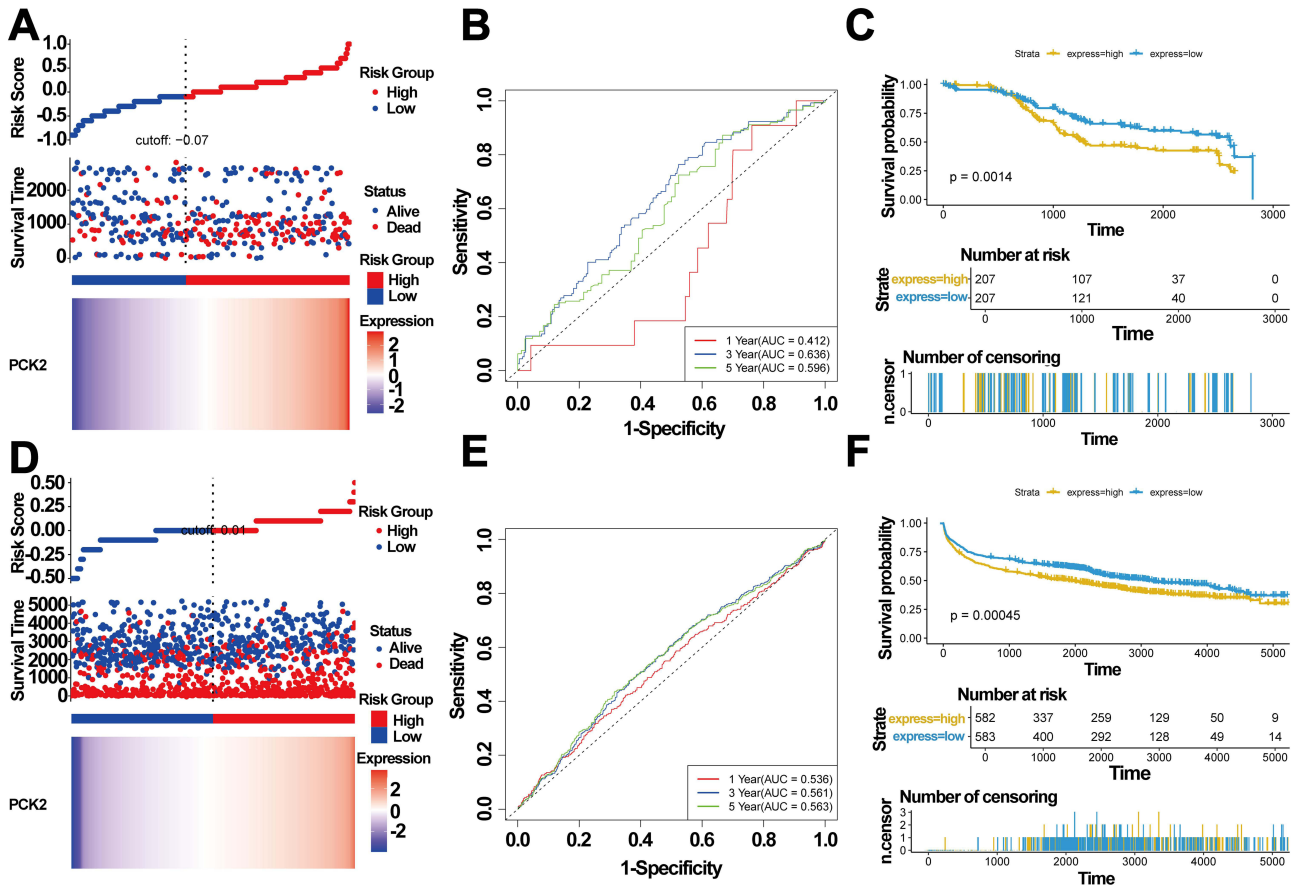

Figure 5 Prognostic significance of *PCK2* in DLBCL. (**A**–**C**) GSE10846 served as the training set. (**A**) *PCK2* expression distribution and corresponding survival status. (**B**) Time-dependent ROC curves for *PCK2* expression in DLBCL. (**C**) Kaplan-Meier survival curve for *PCK2* expression in DLBCL. (**D** - **F**) GSE181063 served as the validation set. (**D**) *PCK2* expression distribution and corresponding survival status. (**E**) Time-dependent ROC curves for *PCK2* expression in DLBCL. (**F**) Kaplan-Meier survival curve for *PCK2* expression in DLBCL.

immune checkpoints can make an impact on DLBCL by regulating the activity of immune cells.[44] The outcome indicated a salient elevation in some of the immunosuppressive molecules (LAG3, PD-L1, VISTA, SIRPA, CD39, CD47) in *PCK2*-High group, while the expression of co-stimulatory molecules ICOS was reduced (Figure 8D).

Correlation Between PCK2 and Immune Cell Infiltration in DLBCL

The immune score can only reflect the intensity of immune response, but not the precise immune cell infiltration status in TIME. Furthermore, ssGSEA algorithm was used to elucidate the complex interactions between *PCK2* and various of immune cells of TIME in DLBCL. Compared with the normal controls, activated $CD8^+$ T cell, activated dendritic cells, macrophage, regulatory T cell (Tregs), and type I T helper cell (Th1) were significantly up-regulated in DLBCL, while the activated B cells and immature B cells were down-regulated (Figure 9A). Notably, contrasted with the *PCK2*-Low group, the immune landscape of *PCK2*-High group was highly consistent with DLBCL (Figure 9B). Furtherly, the results confirmed a direct association between *PCK2* and immunosuppressive cells, such as Myeloid-Derived Suppressor Cells (MDSCs), macrophages and Tregs. Nevertheless, *PCK2* showed a negative association with some immune-promoting cells (activated $CD4^+$ T cells, natural killer cells) (Figure 9C). Lollipop plot displayed the correlations between *PCK2* and 28 type of immune cells (Figure 9D). These findings confirmed that *PCK2* showed an evident correlation with the TIME of DLBCL.

https://doi.org/10.2147/JIR.S548070

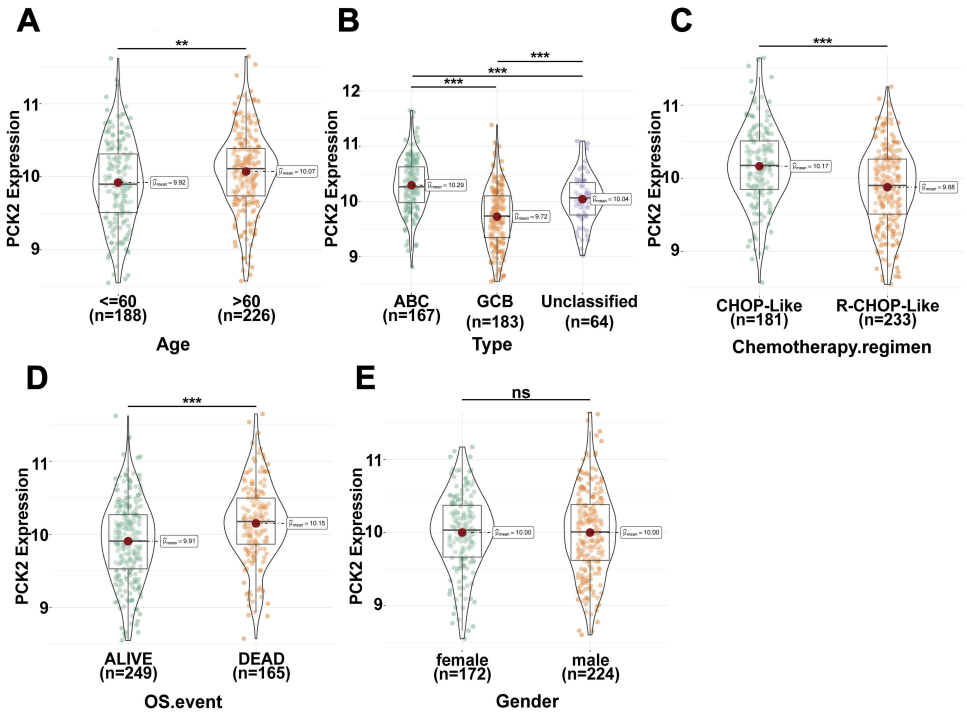

Figure 6 Association of *PCK2* expression with clinical characteristics in DLBCL. (**A**–**E**) The distribution of *PCK2* expression across age, molecular subtype, treatment regimens, OS and sex in DLBCL patients (**p<0.01, ***p<0.001, ns: non-significant).

PCK2 Positively Correlated with IFN_TAMs Infiltration in DLBCL

Our results demonstrated that both IFN-γ and glycolytic pathways exhibited an overall upregulation trend in the *PCK2*-High group using GSEA (Figure 10A and B). Enhanced glycolysis has been clarified as a core catalyst of tumorigenesis.[45] Compared with the *PCK2*-Low group, multiple glycolysis-related genes were highly expressed in PCK2-High group (Figure 10C). IFN_TAMs, a newly identified subset of tumor-associated macrophages (TAMs), integrate interferon response and immune regulatory features. Their phenotype and functions vary across tumor types, reflecting marked heterogeneity.[46] Recent study reported the specific signatures and roles of IFN_TAMs in DLBCL. These cells displayed high glycolytic metabolism and actively shaped an immunosuppressive microenvironment. They were tightly associated with highly malignant B cells and predicted poor prognosis.[8] Given the enrichment of IFN -γ and glycolysis pathways, we next explored the relationship between PCK2 and IFN_TAMs. The results showed that *PCK2*-High group had a high infiltration of IFN_TAMs (Figure 10D), and *PCK2* was notably positively correlated with IFN_TAMs (Figure 10E).

Analysis of PCK2-Interacting Transcriptional Networks in DLBCL

Constructing a co-expression network of *PCK2* to provide new insights for further understanding of its regulatory mechanism and identification of new indicators for DLBCL. Spearman correlation analysis was utilized to explore the top 50 genes related to PCK2, both positively and negatively. STRING database and Cytoscape were utilized to perform Protein-Protein Interaction (PPI) network analysis of the top 50 *PCK2*-related genes (Figure 11A). Based on the PPI Network, we next used the MCODE plugin to explore the top 5 hub genes (SCO2, ISG15, BCS1L, HAUS2, and IFITM3) (Figure 11B). Validation revealed significant overexpression of SCO2, ISG15, BCS1L, and HAUS2 in DLBCL tumor tissues compared to the normal controls, except for IFITM3 (Figure 11C). The evaluate efficacy of 5 hub genes in DLBCL was substantiated by ROC analysis. (Figure 11D).

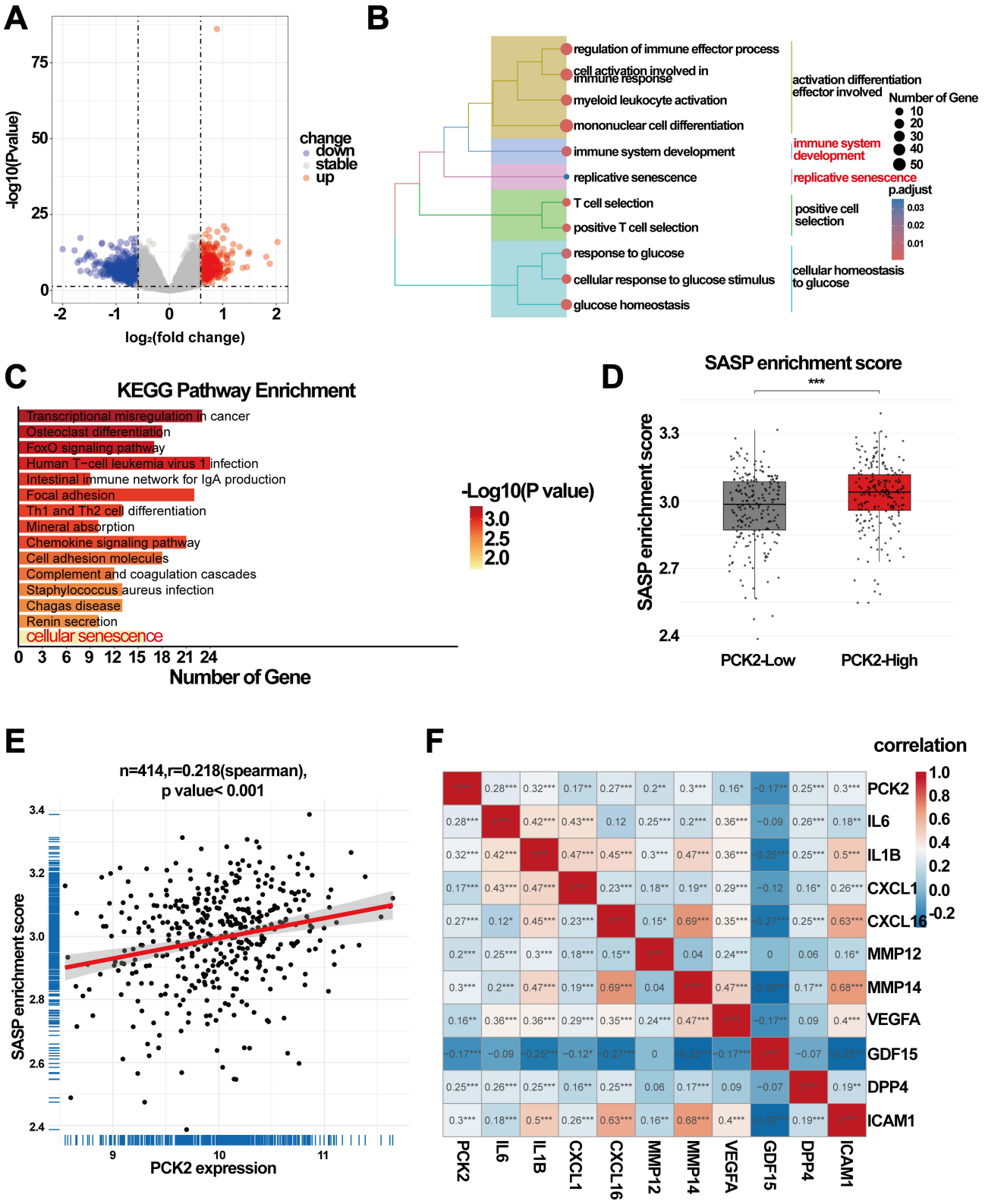

Figure 7 Correlation of *PCK2* with the SASP program in DLBCL. (**A**) The volcano plot displaying the DEGs between two groups. (**B**) GO analysis revealing that DEGs may played a role in multiple process, including senescence pathways. (**C**) KEGG analysis of DEGs. (**D**) Boxplot showing SASP enrichment scores of *PCK2*-High group and *PCK2*-Low group by ssGSEA. (**E**) Scatterplots demonstrating the association of *PCK2* expression with SASP program. (**F**) Heatmap of correlations between *PCK2* and SASP signature molecules (*p<0.05, **p<0.01, ***p<0.001).

https://doi.org/10.2147/JIR.S548070

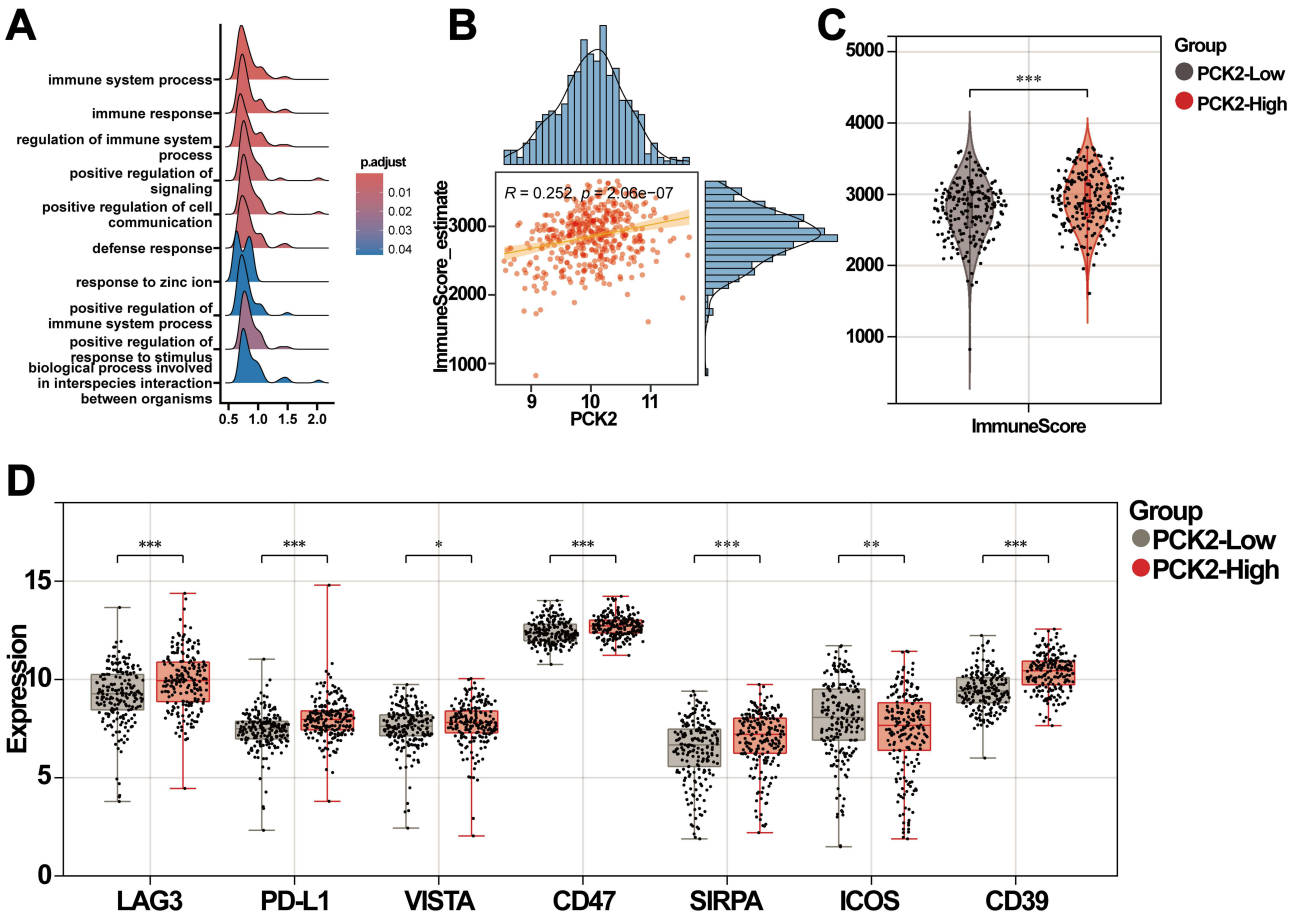

Figure 8 Correlation analysis of *PCK2* with TIME. (**A**) Performed GSEA analysis using genes with |log2 FC| > 0.6, and generated a ridge plot to display the top 10 significant pathways. (**B**) Scatterplots illustrating the positive correlation between *PCK2* expression and immune score. (**C**) Comparison of immune scores between the two groups. (**D**) *PCK2* expression was markedly correlated with immune checkpoints (**p*<0.05, ***p*<0.01, ****p*<0.001).

Validation the Prognostic Value of Genes Exhibiting High Correlation with PCK2 in DLBCL

We further investigated whether the *PCK2*-centered co-expression network exhibited prognostic significance in DLBCL. Univariate analysis of five hub genes confirmed four risk factors (excluding IFITM3) with significant prognostic implications (Figure 12A). Furthermore, the elevated expression of SCO2, ISG15, BCS1L, and HAUS2 correlated with adverse prognosis in DLBCL patients (Figure 12B–F).

Validate the Expression of PCK2 in DLBCL Patients

The exploration of precise biomarkers is aimed at clinical translation. To validate the potential significance of PCK2 in DLBCL, we further applied the immunohistochemical analysis to evaluate the expression of PCK2 in clinical samples. Compared with normal controls, PCK2 was distinctly upregulated in DLBCL, which was highly consistent with our expectation (Figure 13).

Discussion

DLBCL is the most prevalent malignant lymphatic tumor in adults globally. Even with progress in targeted therapies, many patients experiencing relapsed disease still succumb to lymphoma or its complications.[47] Recent studies have shown that the biological and clinical characteristics of DLBCL are affected by both molecular changes within the

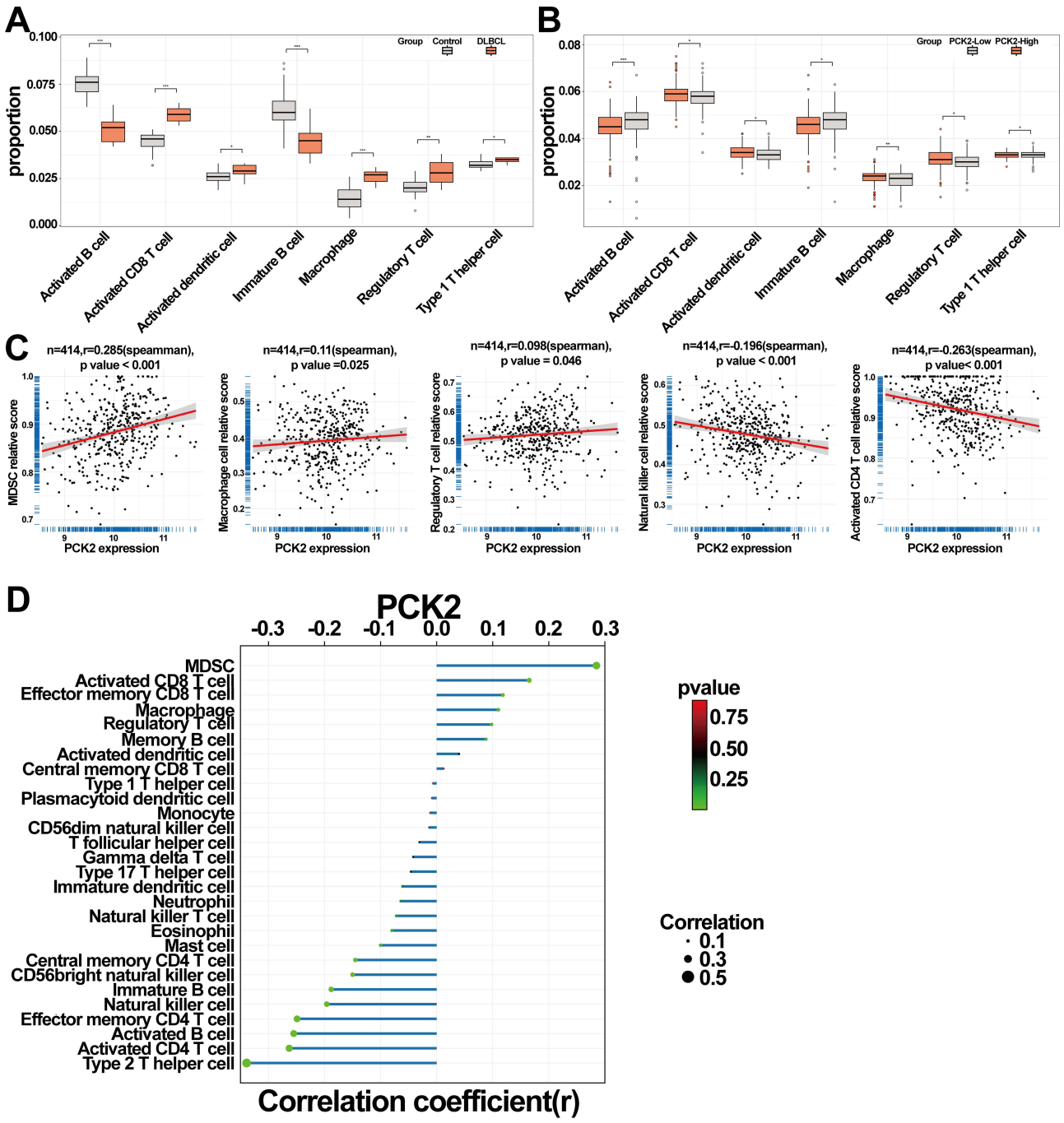

Figure 9 Relationships between *PCK2* expression and immune cell infiltration in DLBCL. (**A**) Comparative analysis of immune cell fractions between control and DLBCL groups. (**B**) Comparative analysis of immune cell proportions in high and low *PCK2* expression groups. (**C**) Scatterplots demonstrating the association of *PCK2* expression with MDSCs, macrophage, Tregs, NK cell, and activated $CD4^+$ T cell. (**D**) The lollipop chart illustrates the correlation coefficient between the immune cells and *PCK2* (*p<0.05, **p<0.01, ***p<0.001).

DLBCL cells and their interactions with the surrounding microenvironment. Studies on DLBCL patients have shown that signal from microenvironmental cells is crucial in disease development and therapeutic effect.[6,48–50]

SASP includes inflammatory factors, chemokines, proteases, and other substances released by senescent cells. These alter the microenvironment, causing chronic inflammation, which accelerates aging and disease progression.[51] Recent studies show that SASP creates an immune escape environment by attracting immunosuppressive cells and causes

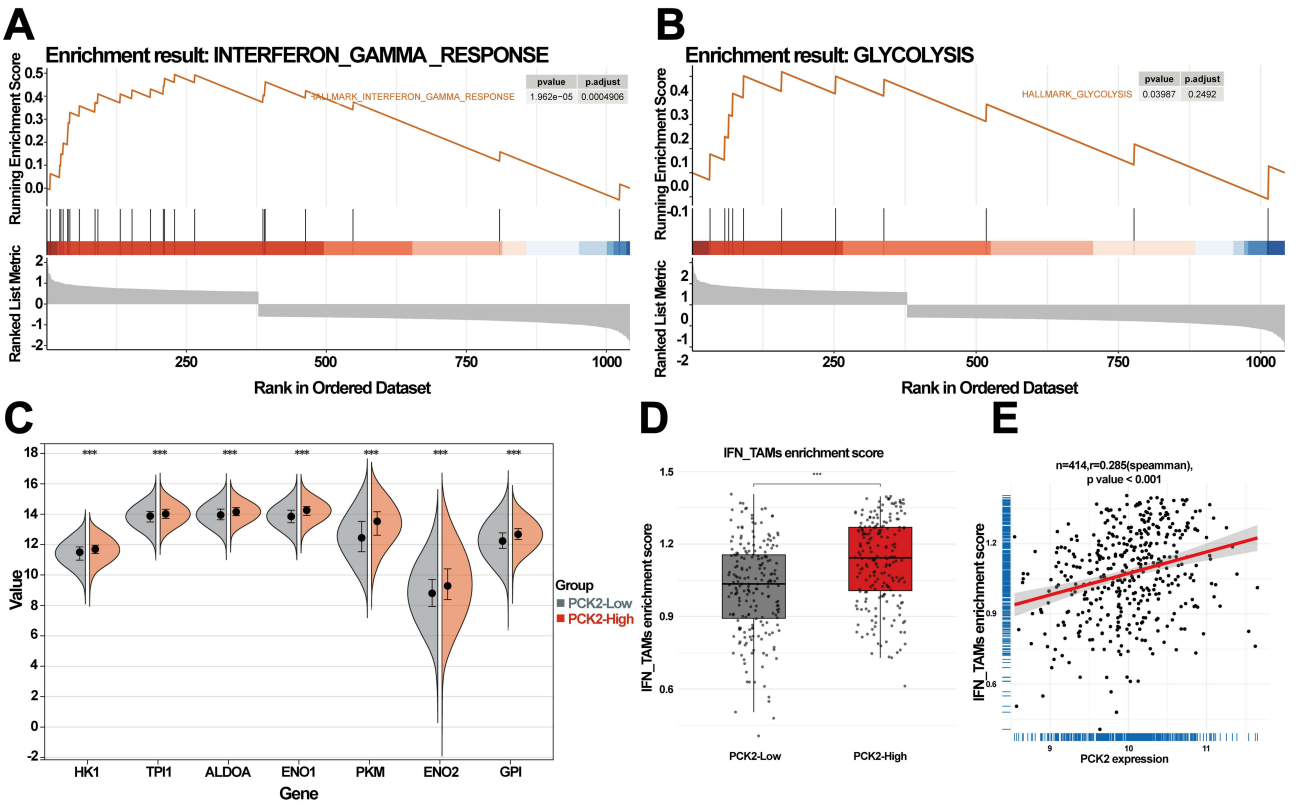

Figure 10 Correlation of *PCK2* with IFN_TAM infiltration in DLBCL. (**A** and **B**) Conduct GSEA analysis using genes with |log2 FC| > 0.6, with the MSigDB dataset as reference. Results indicating significant enrichment of IFN-γ and glycolysis pathway. (**C**) Expression value of key glycolysis pathway genes in *PCK2*-High versus *PCK2*-Low groups. (***p<0.001). (**D**) Boxplot showing IFN_TAMs enrichment scores of *PCK2*-High group and *PCK2*-Low group by ssGSEA. (**E**) Scatterplots demonstrating the association of *PCK2* expression with IFN_TAM infiltration. (***p<0.001).

chronic inflammation through the release of pro-inflammatory factors, ultimately promoting tumor growth.[52–54] Multiple studies have established the SASP program as a functional effector that drives tumor progression. SASP drove progression of IDH wild type glioma by orchestrating the functional states of malignant cells and TAMs.[55] Furthermore, SASP was critical in driving the progression of obesity-associated hepatocellular carcinoma (HCC) in murine models.[56] The influence of SASP on the immune microenvironment in DLBCL and its subsequent impact on the development of DLBCL remains unclear.

This research identified *PCK2* as an independent prognostic indicator with SASP-associated characteristics in DLBCL through a comprehensive analysis. Recent studies have indicated that PCK2 might contribute to the progression of disease.[24,57] We found a distinct association between elevated *PCK2* expression and poor prognosis in DLBCL.

Research indicated that patient age was positively correlated with various features associated with poor DLBCL prognosis.[40] Event-free survival at 24 months (EFS24) serves as a robust indicator for evaluating overall survival in DLBCL.[41] Multivariate analysis revealed that age >60 years remained a significant determinant of post-EFS24 OS relative to the general population.[42] Patients with GCB subtype exhibit both superior OS and progression-free survival compared with ABC subtype patients.[6] Therefore, age >60 years and ABC subtype can be regarded as adverse prognostic features of DLBCL in clinical. We found that *PCK2* was markedly elevated in patients with age>60 and ABC subtype. In treatment aspect, compared with CHOP group, R-CHOP markedly increases the complete remission rate, event-free survival, and overall survival in patients.[43] *PCK2* was markedly lower under R-CHOP treatment than under CHOP alone. These findings indicated that high *PCK2* expression might be linked to the clinically malignant phenotype of DLBCL.

Our results revealed that SASP was significantly elevated in DLBCL patients, suggesting its potential role in the disease. Additionally, *PCK2* was found to be significantly associated with cellular senescence pathway in DLBCL. Given

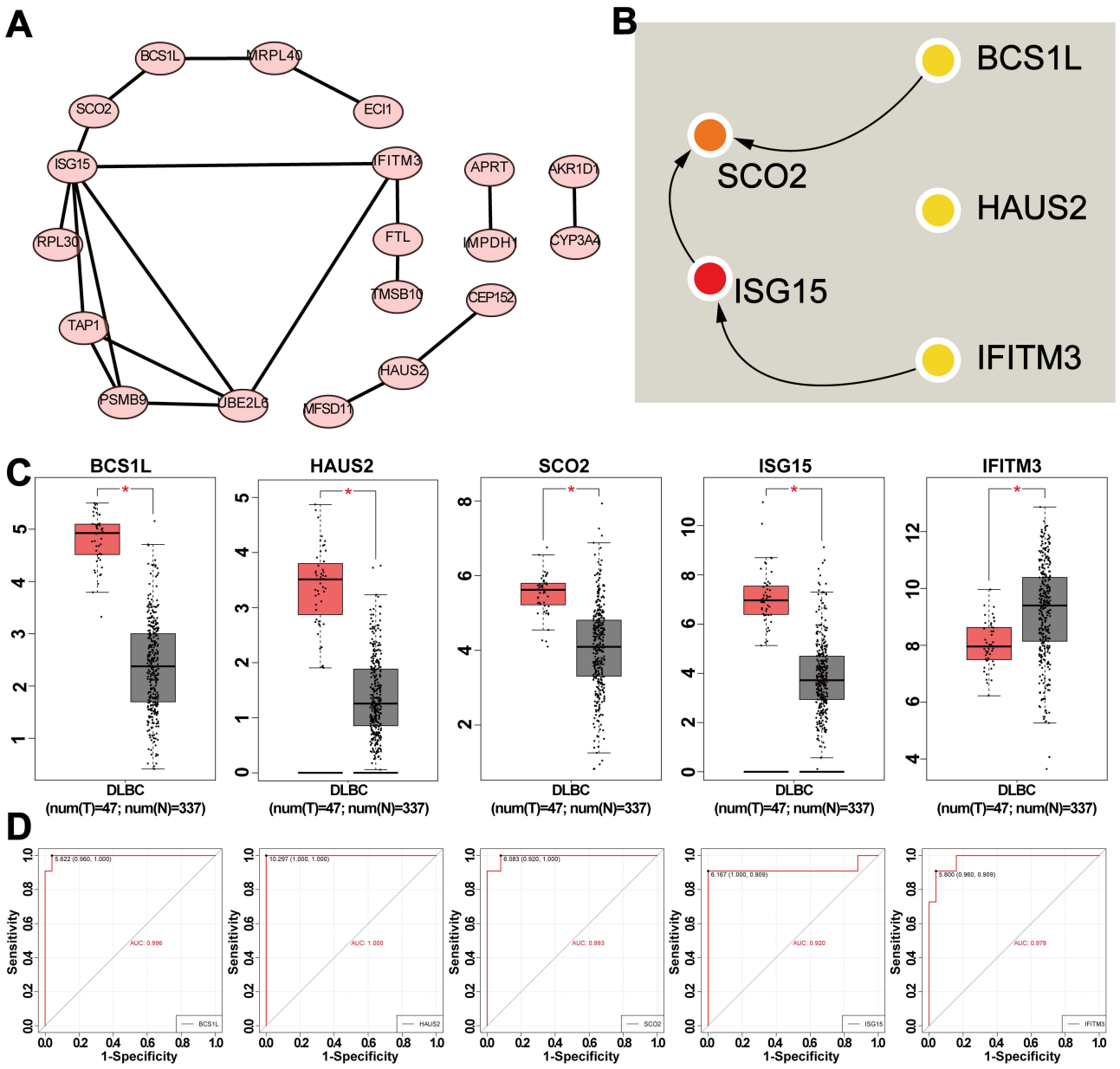

Figure 11 Analysis of genes co-expressed with *PCK2* in DLBCL. (**A**) PPI network of the top 50 *PCK2*-related genes. (**B**) CytoHubba identified five genes. (**C**) The expression levels of five hub genes in both normal and DLBCL groups. (**D**) ROC curve displaying the AUC value of five hub genes. (*$p<0.05$).

that *PCK2* had been identified as an SASP-related gene, the correlation between *PCK2* and SASP program in DLBCL was further investigated. Our results suggested that SASP was markedly activated in *PCK2*-High group. *PCK2* expression was found to be positively related to SASP program, and exhibited distinct associations with multiple core SASP molecules, further indicating a tight linkage between *PCK2* and SASP in DLBCL. Similarly, Tang et al employed bioinformatic approaches to establish a link between *PCK2* and oxidative stress–induced senescence in lung adenocarcinoma.[58] Functional assays by Ma et al confirmed that modulating *PCK2* knockdown in breast cancer cells induced a senescent phenotype and altered the expression of SASP-associated molecules, further substantiating the potential link between *PCK2* and the SASP.[59]

This study found that several glycolysis and immune related pathways were highly enriched in the *PCK2*-high group, indicating that *PCK2* was closely linked to high glycolytic metabolism and TIME in DLBCL. Moreover, the immune

https://doi.org/10.2147/JIR.S548070

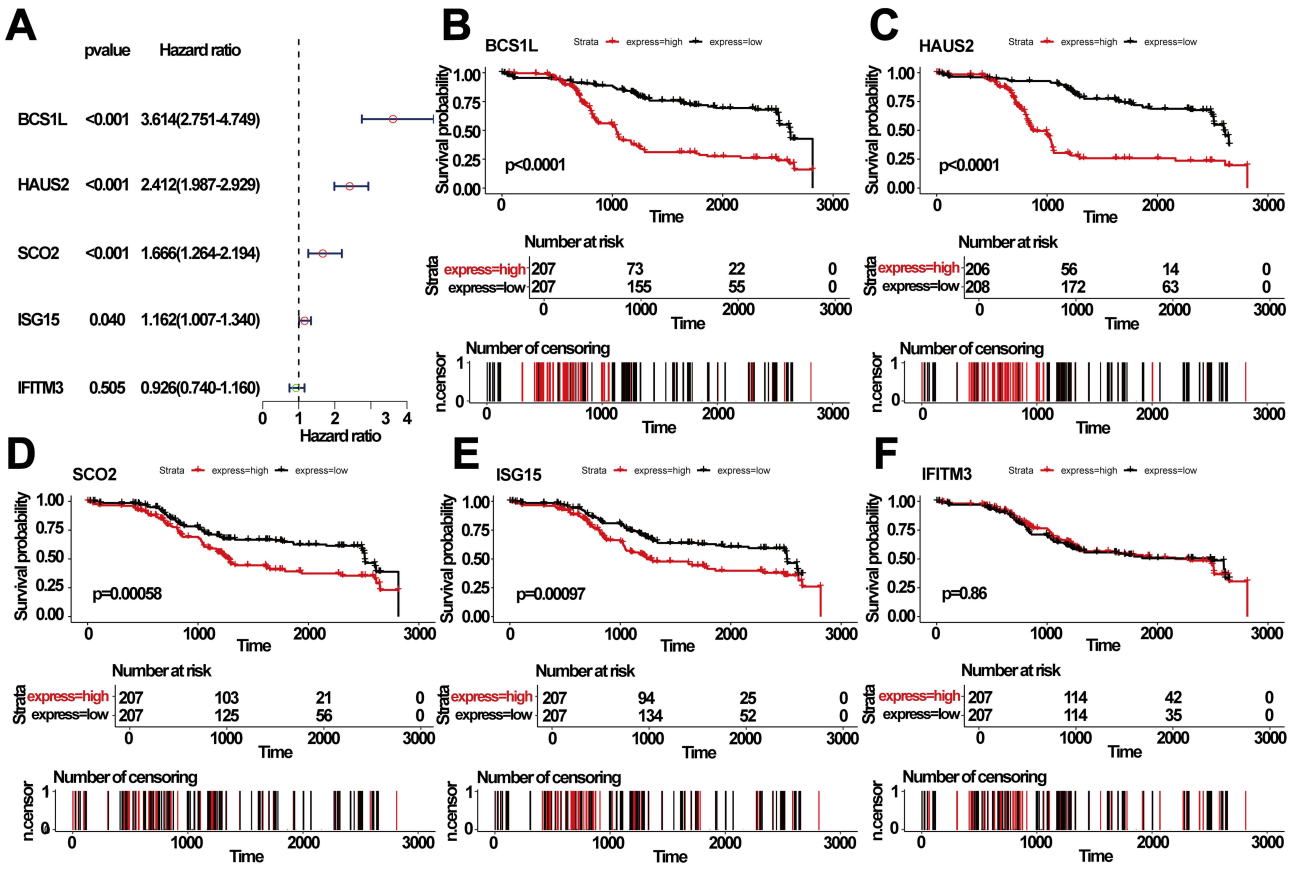

Figure 12 Prognostic value of top five hub genes in DLBCL. (**A**) Forest plot of OS by univariate analysis in DLBCL from GSE10846. (**B**–**F**) Survival curves for BCS1L (**B**), HAUS2 (**C**), SCO2(**D**), ISG15(**E**), and IFITM3 (**F**) in DLBCL from GSE10846.

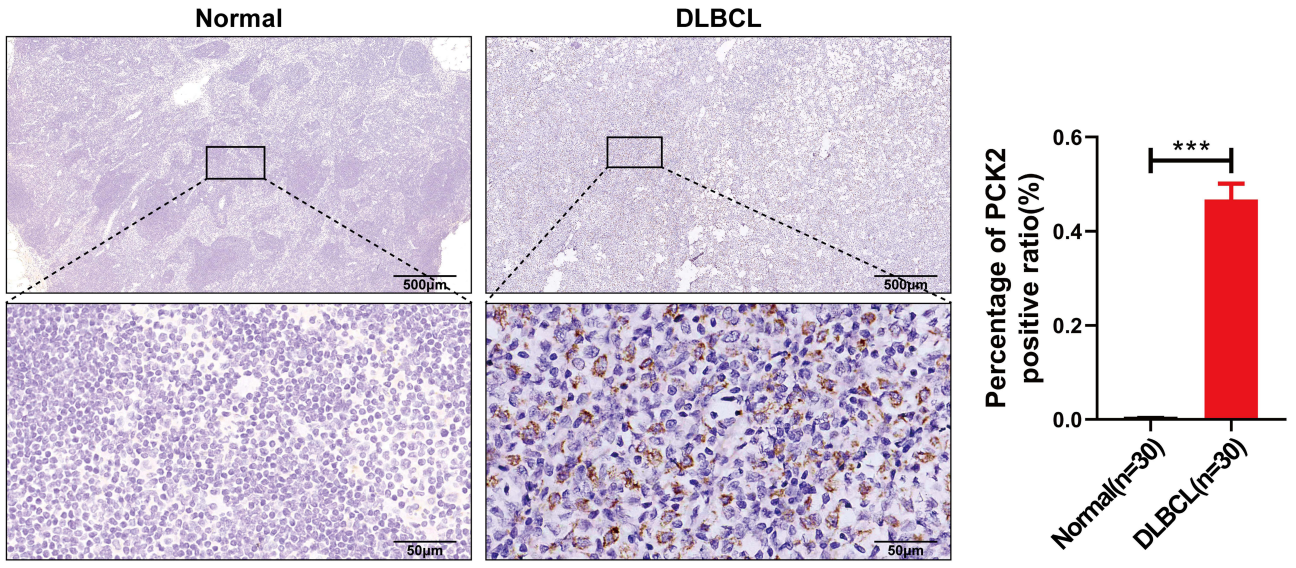

Figure 13 Validation of PCK2 expression in clinical samples, clarified PCK2 protein expression levels in DLBCL and normal tissues using immunohistochemistry (Error bars indicate mean ± SEM, ***p<0.001).

score of the *PCK2*-High group was appreciably higher than *PCK2*-Low group. Enhanced glycolysis is recognized as a key driver of tumor development and progression, influencing malignant growth through various mechanisms.[8,45,60]

TIME plays a crucial role in governing the pathogenesis and therapeutic responsiveness of DLBCL.[8,61] The dynamic interplay between immune cell infiltration and neoplastic immunoediting mechanistically drives tumor microenvironment (TME) remodeling through spatial reorganization of stromal-immune networks and metabolic crosstalk. Immunotherapy, a cutting-edge anticancer approach, works by improving the immune function to eradicate tumor cells. In contrast to traditional cancer treatments like surgery, radiotherapy, and chemotherapy, it has proven to be a highly effective strategy.[62–64] Despite marked therapeutic innovations, current immunotherapeutic modalities for DLBCL remain constrained by intrinsic barriers, including tumor heterogeneity and immune evasion mechanisms, which necessitate comprehensive dissection of the multidimensional crosstalk within the lymphoma-associated immune niche. This study identified a marked association between *PCK2* and immune-related pathways, especially emphasizing the impact of *PCK2* on DLBCL by modulating immune cell activity and the expression of immune checkpoints. We observed that several immunosuppressive molecules, including LAG3, PD-L1, VISTA, SIRPA, CD39, and CD47, were markedly increased in the *PCK2*-High group. The excessive production of these immunosuppressive molecules is directly linked to tumor cells avoiding immune detection.[65–68] To investigate the connection between *PCK2* and tumor immunity, we assessed immune cell infiltration within the TIME of DLBCL. The immune profile of the high *PCK2* expression group closely matches that of DLBCL, indicating that *PCK2* may notably influence the tumor microenvironment in DLBCL. Further analysis revealed that the expression of *PCK2* is directly associated with the infiltration of immunosuppressive cells, such as MDSCs and Tregs, while it is negatively correlated with some immune-promoting cells, such as activated $CD4^+$ T cells and natural killer cells. DLBCL immune escape and disease progression are promoted through multiple mechanisms mediated by MDSCs, macrophages, and Tregs, with their levels closely correlated with disease stage, subtype, and prognosis.[69–73] The findings highlight the prospective significance of *PCK2* in the TIME of DLBCL. In addition, our study uncovered a correlation between *PCK2* and IFN_TAMs infiltration. As a highly heterogeneous TAMs subset, IFN_TAMs in DLBCL were characterized by high glycolytic metabolism, intimate interaction with malignant B cells, and potent immunosuppressive function.[8] Using ssGSEA, we observed a strong positive association between *PCK2* and IFN_TAMs abundance, and *PCK2*-High group exhibited marked enrichment of IFN_TAMs infiltration, further highlighting the link between *PCK2* and the heterogeneous TIME of DLBCL.

We conducted PPI networks analysis for the top 50 *PCK2*-related genes, identifying five central genes—SCO2, ISG15, BCS1L, HAUS2, and IFITM3—with strong prognostic potential in DLBCL. Further analysis indicated that elevated expression of SCO2, ISG15, BCS1L, and HAUS2 is linked to a poorer prognosis in DLBCL patients. Recent studies have revealed that SCO2 fuels tumors through aerobic glycolysis.[74] ISG15 enhances the progression of pancreatic cancer cells, as well as their resistance to Gemcitabine, a standard chemotherapeutic for pancreatic cancer.[51] Collectively, our results indicated that the prognosis of DLBCL may be influenced through synergistic interactions between *PCK2* and the identified hub genes.

Meanwhile, our results suggested that the expression of PCK2 was highly upregulated on tumour tissues, which was further elucidated the potential significance of PCK2 as a candidate indicator for DLBCL.

In conclusion, our findings suggested that *PCK2* might constitute an important molecular feature of DLBCL and could support disease detection and prognostic evaluation. Additionally, although PCK2 has been implicated in various cancers, this study established its association with the specific features of DLBCL, including SASP program, clinical traits and heterogeneous TIME, implying that its function in DLBCL might differ from that in other contexts.

Nevertheless, this study had several limitations. First, the use of publicly available transcriptomic data could have introduced bias attributable to unmeasured confounders. Second, the link between *PCK2* and SASP was inferred solely from bioinformatic analyses; functional assays to establish a direct causal relationship were still lacking and should be prioritized in future work. Finally, although PCK2 had been identified as a key driver in multiple solid tumours, no *PCK2* targeted agent had yet entered pre-clinical or clinical evaluation. Consequently, its therapeutic efficacy and safety remained undefined. The absence of *PCK2* directed strategies and clinical experience represented a major bottleneck for translating experimental observations into clinical applications.

Conclusion

Using comprehensive bioinformatics approaches, we ultimately identified *PCK2* as a SASP-related molecular feature of DLBCL, whose high expression denoted a poor prognosis. Our analyses revealed *PCK2* to be tightly linked to multiple pathogenic processes in DLBCL. On the one hand, Higher *PCK2* levels were markedly enriched among DLBCL patients exhibiting poor prognosis characteristics (eg, ABC subtype, age>60 years). Additionally, SASP signal was markedly elevated in DLBCL patients by ssGSEA, and *PCK2* showed a robust correlation with the SASP program in DLBCL. What's more, *PCK2* was positively correlated with immunosuppressive cell infiltration, particularly the heterogeneous IFN-TAMs. *PCK2* showed negative connected with certain immunostimulatory cell populations. Through the PPI analysis, we identified five hub genes significantly associated with PCK2: SCO2, ISG15, BCS1L, HAUS2, and IFITM3. Elevated expression of SCO2, ISG15, BCS1L, and HAUS2 was linked to poorer prognosis in DLBCL. Finally, through clinical sample validation, compared with healthy controls, the protein expression of PCK2 was significantly elevated in DLBCL patients. In summary, our findings tightly linked *PCK2* to both disease features and prognostic assessment in DLBCL. Notably, these conclusions were bioinformatically inferred, not mechanistically validated, functional assays were still needed to confirm any direct effects.

Data Sharing Statement

All data, analytic methods, and study material are available upon request by contacting the corresponding author.

Ethical Statement and Informed Consent

This study was conducted in accordance with the principles of the Declaration of Helsinki. This study was approved by the Ethics Committee of the Central People's Hospital of Zhanjiang, with approval number PJ[IIT-2021-007-02]. Informed consent was obtained from all subjects involved in the study.

Acknowledgments

The author sincerely thanks the contributors for uploading their datasets and expresses gratitude to the GEO database for providing their platform.

Author Contributions

All authors made a significant contribution to the work reported, whether that is in the conception, study design, execution, acquisition of data, analysis and interpretation, or in all these areas; took part in drafting, revising or critically reviewing the article; gave final approval of the version to be published; have agreed on the journal to which the article has been submitted; and agree to be accountable for all aspects of the work.

Funding

The present study was supported by grants from Guangdong Basic and Applied Basic Research Foundation (2024A1515010858), and Zhanjiang High Level Hospital Construction Project (2021A05155), and Central People's Hospital of Zhanjiang Startup Project of Doctor Scientific Research (2022A08).

Disclosure

The authors declare no potential conflicts of interest in this work.

References

1. Wang SS. Epidemiology and etiology of diffuse large B-cell lymphoma. *Semin Hematol*. 2023;60(5):255–266. doi:10.1053/j.seminhematol.2023.11.004
2. Chapuy B, Stewart C, Dunford AJ, et al. Molecular subtypes of diffuse large B cell lymphoma are associated with distinct pathogenic mechanisms and outcomes. *Nat Med*. 2018;24(5):679–690. doi:10.1038/s41591-018-0016-8
3. Crump M, Neelapu SS, Farooq U, et al. Outcomes in refractory diffuse large B-cell lymphoma: results from the international SCHOLAR-1 study. *Blood*. 2017;130(16):1800–1808. doi:10.1182/blood-2017-03-769620

4. Kanas G, Ge W, Quek RGW, Keeven K, Nersesyan K, Jon EA. Epidemiology of diffuse large B-cell lymphoma (DLBCL) and follicular lymphoma (FL) in the United States and Western Europe: population-level projections for 2020-2025. *Leuk Lymphoma*. 2022;63(1):54–63. doi:10.1080/10428194.2021.1975188
5. Sehn LH, Salles G. Diffuse large B-Cell lymphoma. reply. *N Engl J Med*. 2021;384(23):2262. doi:10.1056/NEJMc2105452
6. Lenz G, Wright G, Dave SS, et al. Stromal gene signatures in large-B-cell lymphomas. *N Engl J Med*. 2008;359(22):2313–2323. doi:10.1056/NEJMoa0802885
7. Nath S, Balling R. The warburg effect reinterpreted 100 yr on: a first-principles stoichiometric analysis and interpretation from the perspective of ATP metabolism in cancer cells. *Function*. 2024;5(3):zqae008. doi:10.1093/function/zqae008
8. Dai L, Fan G, Xie T, et al. Single-cell and spatial transcriptomics reveal a high glycolysis B cell and tumor-associated macrophages cluster correlated with poor prognosis and exhausted immune microenvironment in diffuse large B-cell lymphoma. *Biomark Res*. 2024;12(1):58. doi:10.1186/s40364-024-00605-w
9. Campisi J. Aging, cellular senescence, and cancer. *Annu Rev Physiol*. 2013;75:685–705. doi:10.1146/annurev-physiol-030212-183653
10. Kuilman T, Michaloglou C, Vredeveld LCW, et al. Oncogene-induced senescence relayed by an interleukin-dependent inflammatory network. *Cell*. 2008;133(6):1019–1031. doi:10.1016/j.cell.2008.03.039
11. Saul D, Kosinsky RL, Atkinson EJ, et al. A new gene set identifies senescent cells and predicts senescence-associated pathways across tissues. *Nat Commun*. 2022;13(1):4827. doi:10.1038/s41467-022-32552-1
12. Chibaya L, Snyder J, Ruscetti M. Senescence and the tumor-immune landscape: implications for cancer immunotherapy. *Semin Cancer Biol*. 2022;86(Pt 3):827–845. doi:10.1016/j.semcancer.2022.02.005
13. Guo H, Liu Z, Xu B, et al. Chemokine receptor CXCR2 is transactivated by p53 and induces p38-mediated cellular senescence in response to DNA damage. *Aging Cell*. 2013;12(6):1110–1121. doi:10.1111/acel.12138
14. Orjalo AV, Bhaumik D, Gengler BK, Scott GK, Campisi J. Cell surface-bound IL-1alpha is an upstream regulator of the senescence-associated IL-6/IL-8 cytokine network. *Proc Natl Acad Sci U S A*. 2009;106(40):17031–17036. doi:10.1073/pnas.0905299106
15. Yin K, Patten D, Gough S, et al. Senescence-induced endothelial phenotypes underpin immune-mediated senescence surveillance. *Genes Dev*. 2022;36(9–10):533–549. doi:10.1101/gad.349585.122
16. Al-Khalaf HH, Ghebeh H, Inass R, Aboussekhra A. Senescent breast luminal cells promote carcinogenesis through interleukin-8-dependent activation of stromal fibroblasts. *Mol Cell Biol*. 2019;39(2). doi:10.1128/MCB.00359-18
17. Liu D, Hornsby PJ. Senescent human fibroblasts increase the early growth of xenograft tumors via matrix metalloproteinase secretion. *Cancer Res*. 2007;67(7):3117–3126. doi:10.1158/0008-5472.CAN-06-3452
18. Coppe JP, Patil CK, Rodier F, et al. Senescence-associated secretory phenotypes reveal cell-nonautonomous functions of oncogenic RAS and the p53 tumor suppressor. *PLoS Biol*. 2008;6(12):2853–2868. doi:10.1371/journal.pbio.0060301
19. Dong Z, Luo Y, Yuan Z, Tian Y, Jin T, Xu F. Cellular senescence and SASP in tumor progression and therapeutic opportunities. *Mol Cancer*. 2024;23(1):181. doi:10.1186/s12943-024-02096-7
20. Matsuda S, Revandkar A, Dubash TD, et al. TGF-beta in the microenvironment induces a physiologically occurring immune-suppressive senescent state. *Cell Rep*. 2023;42(3):112129. doi:10.1016/j.celrep.2023.112129
21. Dou X, Fu Q, Long Q, et al. PDK4-dependent hypercatabolism and lactate production of senescent cells promotes cancer malignancy. *Nat Metab*. 2023;5(11):1887–1910. doi:10.1038/s42255-023-00912-w
22. Kim Y, Jang Y, Kim MS, Kang C. Metabolic remodeling in cancer and senescence and its therapeutic implications. *Trends Endocrinol Metab*. 2024;35(8):732–744. doi:10.1016/j.tem.2024.02.008
23. Wang B, Han J, Elisseeff JH, Demaria M. The senescence-associated secretory phenotype and its physiological and pathological implications. *Nat Rev Mol Cell Biol*. 2024;25(12):958–978. doi:10.1038/s41580-024-00727-x
24. Montal ED, Dewi R, Bhalla K, et al. PEPCK coordinates the regulation of central carbon metabolism to promote cancer cell growth. *Mol Cell*. 2015;60(4):571–583. doi:10.1016/j.molcel.2015.09.025
25. Vincent EE, Sergushichev A, Griss T, et al. Mitochondrial phosphoenolpyruvate carboxykinase regulates metabolic adaptation and enables glucose-independent tumor growth. *Mol Cell*. 2015;60(2):195–207. doi:10.1016/j.molcel.2015.08.013
26. Lu Y, Zhu J, Zhang Y, et al. Lactylation-driven IGF2BP3-mediated serine metabolism reprogramming and RNA m6A-modification promotes lenvatinib resistance in HCC. *Adv Sci (Weinh)*. 2024;11(46):e2401399. doi:10.1002/advs.202401399
27. Hsu HP, Chu PY, Chang TM, et al. Mitochondrial phosphoenolpyruvate carboxykinase promotes tumor growth in estrogen receptor-positive breast cancer via regulation of the mTOR pathway. *Cancer Med*. 2023;12(2):1588–1601. doi:10.1002/cam4.4969
28. Li C, Zhang ED, Ye Y, Xiao Z, Huang H, Zeng Z. Association of mitochondrial phosphoenolpyruvate carboxykinase with prognosis and immune regulation in hepatocellular carcinoma. *Sci Rep*. 2024;14(1):14051. doi:10.1038/s41598-024-64907-7
29. Brune V, Tiacci E, Pfeil I, et al. Origin and pathogenesis of nodular lymphocyte-predominant Hodgkin lymphoma as revealed by global gene expression analysis. *J Exp Med*. 2008;205(10):2251–2268. doi:10.1084/jem.20080809
30. Lacy SE, Barrans SL, Beer PA, et al. Targeted sequencing in DLBCL, molecular subtypes, and outcomes: a haematological malignancy research network report. *Blood*. 2020;135(20):1759–1771. doi:10.1182/blood.2019003535
31. Zhang X, Wen Z, Wang Q, Ren L, Zhao S. A novel stratification framework based on anoikis-related genes for predicting the prognosis in patients with osteosarcoma. *Front Immunol*. 2023;14:1199869. doi:10.3389/fimmu.2023.1199869
32. Chunxiao L, Xin H, Bowen L, et al. Uncovering the mechanism of resveratrol in the treatment of asthma: a network pharmacology approach with molecular docking and experimental validation. *Front Pharmacol*. 2025;16:1596737. doi:10.3389/fphar.2025.1596737
33. Ma S, Dai Y. Principal component analysis based methods in bioinformatics studies. *Brief Bioinform*. 2011;12(6):714–722. doi:10.1093/bib/bbq090
34. McCarthy DJ, Smyth GK. Testing significance relative to a fold-change threshold is a TREAT. *Bioinformatics*. 2009;25(6):765–771. doi:10.1093/bioinformatics/btp053
35. Yu G, Wang LG, Han Y, He QY. clusterProfiler: an R package for comparing biological themes among gene clusters. *OMICS*. 2012;16(5):284–287. doi:10.1089/omi.2011.0118
36. Langfelder P, Horvath S. WGCNA: an R package for weighted correlation network analysis. *BMC Bioinf*. 2008;9:559. doi:10.1186/1471-2105-9-559

37. Robin X, Turck N, Hainard A, et al. pROC: an open-source package for R and S+ to analyze and compare ROC curves. *BMC Bioinf*. 2011;12:77. doi:10.1186/1471-2105-12-77
38. Yoshihara K, Shahmoradgoli M, Martinez E, et al. Inferring tumour purity and stromal and immune cell admixture from expression data. *Nat Commun*. 2013;4:2612. doi:10.1038/ncomms3612
39. Hanzelmann S, Castelo R, Guinney J. GSVA: gene set variation analysis for microarray and RNA-seq data. *BMC Bioinf*. 2013;14:7. doi:10.1186/1471-2105-14-7
40. Klapper W, Kreuz M, Kohler CW, et al. Patient age at diagnosis is associated with the molecular characteristics of diffuse large B-cell lymphoma. *Blood*. 2012;119(8):1882–1887. doi:10.1182/blood-2011-10-388470
41. Maurer MJ, Ghesquieres H, Jais JP, et al. Event-free survival at 24 months is a robust end point for disease-related outcome in diffuse large B-cell lymphoma treated with immunochemotherapy. *J Clin Oncol*. 2014;32(10):1066–1073. doi:10.1200/JCO.2013.51.5866
42. Abu Sabaa A, Morth C, Hasselblom S, et al. Age is the most important predictor of survival in diffuse large B-cell lymphoma patients achieving event-free survival at 24 months: a Swedish population-based study. *Br J Haematol*. 2021;193(5):906–914. doi:10.1111/bjh.17206
43. Coiffier B, Lepage E, Briere J, et al. CHOP chemotherapy plus rituximab compared with CHOP alone in elderly patients with diffuse large-B-cell lymphoma. *N Engl J Med*. 2002;346(4):235–242. doi:10.1056/NEJMoa011795
44. Butler MJ, Aguiar RCT. Biology informs treatment choices in diffuse large B cell lymphoma. *Trends Cancer*. 2017;3(12):871–882. doi:10.1016/j.trecan.2017.09.008
45. Li X, Yang Y, Zhang B, et al. Lactate metabolism in human health and disease. *Signal Transduct Target Ther*. 2022;7(1):305. doi:10.1038/s41392-022-01151-3
46. Qian Y, Yin Y, Zheng X, Liu Z, Wang X. Metabolic regulation of tumor-associated macrophage heterogeneity: insights into the tumor microenvironment and immunotherapeutic opportunities. *Biomark Res*. 2024;12(1):1. doi:10.1186/s40364-023-00549-7
47. Frontzek F, Lenz G. Novel insights into the pathogenesis of molecular subtypes of diffuse large B-cell lymphoma and their clinical implications. *Expert Rev Clin Pharmacol*. 2019;12(11):1059–1067. doi:10.1080/17512433.2019.1683447
48. Cayrol F, Díaz Flaqué MC, Fernando T, et al. Integrin αvβ3 acting as membrane receptor for thyroid hormones mediates angiogenesis in malignant T cells. *Blood*. 2015;125(5):841–851. doi:10.1182/blood-2014-07-587337
49. Mourcin F, Pangault C, Amin-Ali R, Amé-Thomas P, Tarte K. Stromal cell contribution to human follicular lymphoma pathogenesis. *Front Immunol*. 2012;3:280. doi:10.3389/fimmu.2012.00280
50. Ciavarella S, Vegliante MC, Fabbri M, et al. Dissection of DLBCL microenvironment provides a gene expression-based predictor of survival applicable to formalin-fixed paraffin-embedded tissue. *Ann Oncol*. 2018;29(12):2363–2370. doi:10.1093/annonc/mdy450
51. Meng Y, Bian L, Zhang M, et al. ISG15 promotes progression and gemcitabine resistance of pancreatic cancer cells through ATG7. *Int J Biol Sci*. 2024;20(4):1180–1193. doi:10.7150/ijbs.85424
52. Pereira BI, Devine OP, Vukmanovic-Stejic M, et al. Senescent cells evade immune clearance via HLA-E-mediated NK and CD8+ T cell inhibition. *Nat Commun*. 2019;10(1):2387. doi:10.1038/s41467-019-10335-5
53. Muñoz DP, Yannone SM, Daemen A, et al. Targetable mechanisms driving immunoevasion of persistent senescent cells link chemotherapy-resistant cancer to aging. *JCI Insight*. 2019;5(14). doi:10.1172/jci.insight.124716
54. Ruhland MK, Loza AJ, Capietto A-H, et al. Stromal senescence establishes an immunosuppressive microenvironment that drives tumorigenesis. *Nat Commun*. 2016;7:11762. doi:10.1038/ncomms11762
55. Liu Y, Feng Y, Cheng L, Xu Y, Wu A, Cheng P. Profiling with senescence-associated secretory phenotype score identifies GDC-0879 as a small molecule sensitizing glioblastoma to anti-PD1. *Cell Death Dis*. 2025;16(1):602. doi:10.1038/s41419-025-07915-3
56. Yoshimoto S, Loo TM, Atarashi K, et al. Obesity-induced gut microbial metabolite promotes liver cancer through senescence secretome. *Nature*. 2013;499:7456):97–101. doi:10.1038/nature12347
57. Méndez-Lucas A, Hyroššová P, Novellasdemunt L, Viñals F, Perales JC. Mitochondrial phosphoenolpyruvate carboxykinase (PEPCK-M) is a pro-survival, endoplasmic reticulum (ER) stress response gene involved in tumor cell adaptation to nutrient availability. *J Biol Chem*. 2014;289(32):22090–22102. doi:10.1074/jbc.M114.566927
58. Tang M, Sun J, Cai Z. PCK2 inhibits lung adenocarcinoma tumor cell immune escape through oxidative stress-induced senescence as a potential therapeutic target. *J Thorac Dis*. 2023;15(5):2601–2615. doi:10.21037/jtd-23-542
59. Ma X, Gao Y, Liu J, et al. Low expression of PCK2 in breast tumors contributes to better prognosis by inducing senescence of cancer cells. *IUBMB Life*. 2022;74(9):896–907. doi:10.1002/iub.2651
60. Wang J-Z, Zhu W, Han J, et al. The role of the HIF-1α/ALYREF/PKM2 axis in glycolysis and tumorigenesis of bladder cancer. *Cancer Commun*. 2021;41(7):560–575. doi:10.1002/cac2.12158
61. Wright GW, Huang DW, Phelan JD, et al. A probabilistic classification tool for genetic subtypes of diffuse large B cell lymphoma with therapeutic implications. *Cancer Cell*. 2020;37(4). doi:10.1016/j.ccell.2020.03.015
62. Melchardt T, Egle A, Greil R. How I treat diffuse large B-cell lymphoma. *ESMO Open*. 2023;8(1):100750. doi:10.1016/j.esmoop.2022.100750
63. Rui R, Zhou L, He S. Cancer immunotherapies: advances and bottlenecks. *Front Immunol*. 2023;14:1212476. doi:10.3389/fimmu.2023.1212476
64. Ma S, Li X, Wang X, et al. Current progress in CAR-T cell therapy for solid tumors. *Int J Biol Sci*. 2019;15(12):2548–2560. doi:10.7150/ijbs.34213
65. Ma J, Pang X, Li J, Zhang W, Cui W. The immune checkpoint expression in the tumor immune microenvironment of DLBCL: clinicopathologic features and prognosis. *Front Oncol*. 2022;12:1069378. doi:10.3389/fonc.2022.1069378
66. Keane C, Law SC, Gould C, et al. LAG3: a novel immune checkpoint expressed by multiple lymphocyte subsets in diffuse large B-cell lymphoma. *Blood Adv*. 2020;4(7):1367–1377. doi:10.1182/bloodadvances.2019001390
67. Biedermann A, Patra-Kneuer M, Mougiakakos D, et al. Blockade of the CD47/SIRPα checkpoint axis potentiates the macrophage-mediated antitumor efficacy of tafasitamab. *Haematologica*. 2024;109(12):3928–3940. doi:10.3324/haematol.2023.284795
68. Beer SA, Went M, Mills C, et al. Mendelian randomization of immune cell phenotypes to discover potential drug targets for B-cell malignancy. *Blood Cancer J*. 2025;15(1):62. doi:10.1038/s41408-025-01277-x
69. Wang Z, Jiang R, Li Q, Wang H, Tao Q, Zhai Z. Elevated M-MDSCs in circulation are indicative of poor prognosis in diffuse large B-cell lymphoma patients. *J Clin Med*. 2021;10(8). doi:10.3390/jcm10081768
70. Wang H-Y, Yang F-C, Yang C-F, et al. Surface TREM2 on circulating M-MDSCs as a novel prognostic factor for adults with treatment-naïve diffuse large B-cell lymphoma. *Exp Hematol Oncol*. 2023;12(1):35. doi:10.1186/s40164-023-00399-x

71. Huang Y-H, Cai K, Xu -P-P, et al. CREBBP/EP300 mutations promoted tumor progression in diffuse large B-cell lymphoma through altering tumor-associated macrophage polarization via FBXW7-NOTCH-CCL2/CSF1 axis. *Signal Transduct Target Ther*. 2021;6(1):10. doi:10.1038/s41392-020-00437-8
72. Shao R, Liu C, Xue R, et al. Tumor-derived exosomal ENO2 modulates polarization of tumor-associated macrophages through reprogramming glycolysis to promote progression of diffuse Large B-cell lymphoma. *Int J Biol Sci*. 2024;20(3):848–863. doi:10.7150/ijbs.91154
73. Su X, Sun T, Li M, et al. Lkb1 aggravates diffuse large B-cell lymphoma by promoting the function of Treg cells and immune escape. *J Transl Med*. 2022;20(1):378. doi:10.1186/s12967-022-03588-0
74. Matoba S, Kang J-G, Patino WD, et al. p53 regulates mitochondrial respiration. *Science*. 2006;312(5780):1650–1653.